

# Propofol produces neurotoxicity by inducing mitochondrial apoptosis

YUBING LIANG<sup>1,2\*</sup>, YU HUANG<sup>1,2\*</sup>, RONGGE SHAO<sup>1,2\*</sup>, FEI XIAO<sup>3</sup>,  
FEI LIN<sup>1,2</sup>, HUIJUN DAI<sup>1,2</sup> and LINGHUI PAN<sup>1,2</sup>

<sup>1</sup>Department of Anesthesiology, Guangxi Medical University Cancer Hospital; <sup>2</sup>Perioperative Medicine Research Center, Guangxi Medical University Cancer Hospital, Guangxi Key Laboratory for Basic Science and Prevention of Perioperative Organ Disfunction; <sup>3</sup>Department of Anesthesiology, The First Affiliated Hospital of Guangxi Medical University, Nanning, Guangxi Zhuang Autonomous Region 530021, P.R. China

Received May 25, 2021; Accepted May 10, 2022

DOI: 10.3892/etm.2022.11567

**Abstract.** Propofol is a fast and short-acting intravenous anesthetic widely used in clinical anesthesia and intensive care unit sedation. However, its use can cause abnormal effects on the central nervous system. Thus, the purpose of this study was to investigate the mechanism of propofol on primary hippocampal neuron injury. In addition, we aimed to determine whether a correlation exists between propofol and mitochondrial apoptosis-induced neurotoxicity. Hippocampal neurons cultured for 4 days were exposed to different drugs. The treatment groups were divided according to drug exposure into propofol, a rotenone inhibitor, and a coenzyme Q10 agonist groups. The final concentrations of propofol were 1, 10 and 100  $\mu$ M. The content of ATP and reactive oxygen species (ROS) in the neurons of each group were detected using commercial kits in the culture supernatant after 3 h of drug exposure. Western blotting was used to analyze the expression of apoptosis-related proteins. The JC-1 kit was used to detect the mitochondrial membrane potential. The results revealed that, compared with the non-propofol treatment groups, the expression of apoptosis-related proteins, ATP content, and mitochondrial membrane potential were significantly decreased while the ROS content was markedly increased in the propofol treatment group. In conclusion, propofol treatment promoted damage to hippocampal neuronal mitochondria in a dose-dependent manner. This damage may

lead to neuronal apoptosis and neurotoxicity by inducing the inhibition of mitochondrial respiratory chain complex I.

## Introduction

Mitochondria, important semi-autonomous organelles, are the 'power plant' for cellular activities. They are the main sites for energy conversion, regulation of redox potential energy, and signal transduction. Additionally, mitochondria are important sites for the generation of reactive oxygen species (ROS), apoptosis regulation, and selective gene expression (1,2). Although the molecular structures of anesthetics are usually different, most can cause changes in multiple functions at the mitochondrial level (3). For example, the occurrence of propofol infusion syndrome (PRIS) is hypothesized to result from direct interference with mitochondrial respiratory chains or hindrance of fatty acid oxidation-related functions (4).

Propofol is an alkylphenolic compound and a mild proton carrier (protonophore), different from dinitrophenols (uncouplers). Propofol impairs respiratory chain complex I and complex III activities (5) and induces reduced mitochondrial complex II and complex IV activity (6). Long-term and high-dose infusions of propofol can inhibit the electron transport chain flow in myocardial mitochondria, as well as hinder energy production, finally causing metabolic acidosis, arrhythmia, and other clinical symptoms (7). However, few studies have explored the mechanisms of propofol on mitochondrial energy metabolism dynamics in hippocampal neurons.

Cytochrome *c* (CytC) is a basic component of the respiratory chain and results from the synthesis of pro-cytochrome *c* and heme from two inactive precursor molecules (8). CytC deficiencies can lead to blockage of electron transport chain functions due to overproduction of reactive oxygen species (ROS) and incomplete oxidation, reduced ATP synthesis, and apoptosis induction (9). Increasing evidence suggests that CytC is a universally recognized mitochondrial-originated cell death signal. Recent research has found that mitochondrial CytC regulates apoptosis by facilitating and amplifying apoptotic signals (10).

The CytC/Apaf 1/caspase-9 complex is known as the 'apoptosome'. Activated caspase in apoptotic bodies continuously

---

*Correspondence to:* Dr Yubing Liang or Dr Linghui Pan, Department of Anesthesiology, Guangxi Medical University Cancer Hospital, 71 Hedi Road, Nanning, Guangxi Zhuang Autonomous Region 530021, P.R. China  
E-mail: liangybstugxmu.edu@163.com  
E-mail: panlinghui@gxmu.edu.cn

\*Contributed equally

**Key words:** propofol, hippocampal neurons, apoptosis-related protein, neurotoxicity

activates downstream caspase-3, thereby triggering a cascading reaction leading to apoptosis (11). Research using recently developed techniques has found that CytC, Apaf1, and dATP are synergistic factors required to activate caspase-9. In addition, CytC release was found to increase ROS production and mediate apoptosis by causing electron transport disorders in the mitochondrial respiratory chain (12). Additionally, a third influential pathway in apoptotic signaling has recently been proposed: the endoplasmic reticulum stress pathway. The dynamics of this pathway can cause calcium release from the endoplasmic reticulum, lead to imbalances in calcium homeostasis in the cytoplasm, activate caspase, and mediate apoptosis (13).

Moreover, quantitative assessments have indicated that the application of 50  $\mu\text{mol/l}$  propofol can cause CytC release in HL-60 cells, and subsequently promote the expression of cleavage products from the apoptotic protein Bid, suggesting that propofol can activate mitochondrial-related apoptotic pathways (14). Although CytC losses increase with higher propofol concentrations, they do not interfere with mitochondrial apoptotic-related pathways at relatively low concentrations (15).

Based on these findings and current clinical needs, we aimed to assess the mechanisms of propofol neurotoxicity during development. More specifically, we examined mitochondrial damage in primary hippocampal neurons of rats, and whether this process could be reversed by respiratory chain inhibitors. By examining the mechanisms and roles of propofol in neuronal apoptosis, we aim to establish a better theoretical basis and provide increasingly precise guidance for clinical applications of brain protection drugs to antagonize the neurotoxicity of propofol.

## Materials and methods

*Establishment of a primary culture of hippocampal neurons from neonatal rats.* The experimental procedures and protocols were approved by the Animal Use and Care Committee of the Guangxi Medical University (no. SCXK GUI 2004-0002) and were performed following the Guangxi Medical University's Guideline for Ethical Review of Animal Welfare (GB/T 35892-2018). A total of 78 Neonatal SD rats (one day old) obtained from animal center of Guangxi Medical University were sacrificed by neck rupture. Brain tissues were quickly placed upon ice-cooled plates and separated using anatomical microscopy. Then, hippocampal tissue specimens were submerged in a precooled HBSS solution and washed. Tissues were cut with scissors and digested with a 0.125% trypsin reaction terminated after 15 min. Placental blue staining was used for cell counting, and hippocampal neurons were transferred to 6-well plates, 96-well plates, and 50-ml culture flasks at  $2\text{--}3 \times 10^5$  cells/ml. Cells were cultured in an incubator set at 37°C in 5%  $\text{CO}_2$  atmosphere. After 48 h, and every 2 days thereafter, the supernatants were replaced, and cell growth was assessed using phase-contrast microscopy. Cultured hippocampal neurons were identified by NSE primary antibody immunofluorescence staining (cat# ab79757 Abcam) at day 7.

*Experimental groups and processing.* After culturing primary hippocampal neurons *in vitro*, neurons gradually outgrew

axons and dendrites and subsequently formed axonal connections. Hippocampal neurons were divided into control (C), 0.25% dimethyl sulfoxide (DMSO) (D), fat emulsion (F), propofol 1  $\mu\text{M}$  (P1), propofol 10  $\mu\text{M}$  (P10), and propofol 100  $\mu\text{M}$  (P100) groups. All medication groups were exposed for 3 h for subsequent analyses.

To examine whether propofol produces neurotoxicity by inhibiting the mitochondrial respiratory chain, hippocampal neurons were divided into control (C), fat emulsion (F), 0.25% DMSO (D), propofol 100  $\mu\text{M}$  (P), rotenone inhibitor 0.1  $\mu\text{M}$  (I), Coenzyme Q10 10  $\mu\text{M}$  (CQ), Coenzyme Q10 10  $\mu\text{M}$  + propofol 100  $\mu\text{M}$  (PCQ) groups (Fig. 1). Neuronal cells in groups C, F and D were incubated with fresh medium, fat emulsion, and 0.25% DMSO, respectively. Neuronal cells in group P were incubated with 100  $\mu\text{M}$  propofol for 3 h; neuronal cells in group I were incubated with 0.1  $\mu\text{M}$  mitochondrial complex enzyme I rotenone inhibitor for 1 h; the CQ group was treated with 10  $\mu\text{M}$  Coenzyme Q10 agonist for 2 h; the PCQ group was first treated with 10  $\mu\text{M}$  Coenzyme Q10 for 2 h, and then with 100  $\mu\text{M}$  propofol for 3 h. Each group of test samples was performed in triplicate, and each treatment group had at least three independently assessed batches of samples.

*Western blotting.* Cell samples from each group were lysed with precooled RIPA lysis buffer and incubated on ice for 20 min. The supernatant was collected after centrifuging the sample two times at  $12,000 \times g$  for 15 min at 4°C. Then, protein samples were used for 10% SDS-PAGE electrophoresis. Separated proteins were wetly transferred to PVDF membranes, confirmed by ponceau red staining. Next, the membrane was blocked in 3% BSA-TBST at room temperature in a shaker for 30 min, followed by washes with TBST. Primary antibodies (Bcl-2; cat. no. ab32124), (Apaf-1; cat. no. ab234436), (Bax; cat. no. ab32503), (cleaved caspase-9; cat. no. ab2324), (CytC; cat. no. ab133504) obtained from Abcam and diluted to 1:1,000 were added to the membrane and incubated at 4°C overnight. HRP goat anti-rabbit IgG (H+L) obtained from Abcam and diluted 1:1,000 (cat. no. ab6721) in 5% skimmed milk powder-TBST was used as a secondary antibody, at room temperature for 1 h. The ECL luminescent solution was added to the film and allowed to react for 3–5 min. The film was exposed for 10–300 sec, developed for 2 min, and then fixed. Finally, image analyses were performed using LabWorks 4.6 Image Analysis Software (LabWorks).

*Mitochondrial membrane potential assessed by JC-1 staining.* Qualitative measures of mitochondrial membrane potential were assessed by JC-1 staining. Cells were stained with JC-1 on a 6-well culture plate, and then observed under confocal microscopy. Red to green fluorescence ratios represented mitochondrial membrane potential and were analyzed using cationic lipid fluorescent JC-1 staining.

JC-1 (2.5  $\mu\text{g/ml}$ ) was added to the cell suspension until a uniform red-purple color emerged. When the mitochondrial membrane potential is high, JC-1 can gather in the mitochondrial matrix to form polymers (J-aggregates) and produce red fluorescence. When the mitochondrial membrane potential is low, JC-1 cannot gather in the mitochondrial matrix, thus JC-1 is a monomer and produces green fluorescence. Next, the

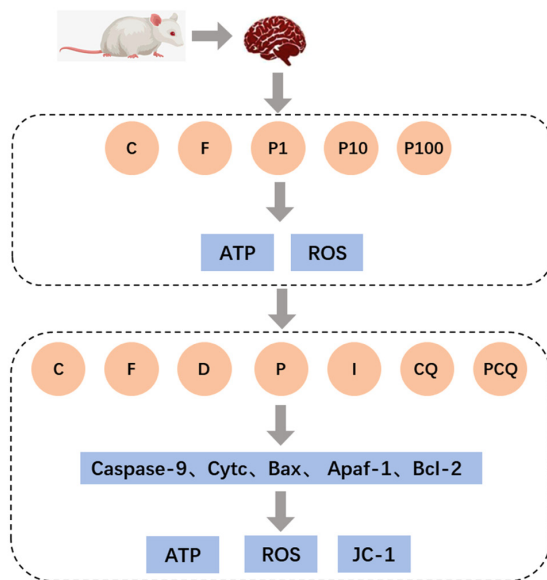


Figure 1. Experimental groups and processes. C, Control group; F, Fat emulsion group; P1, 1  $\mu$ M propofol group; P10, 10  $\mu$ M propofol group; P100, 100  $\mu$ M propofol group. D, 0.25% DMSO; P, treatment with 100  $\mu$ M propofol for 3 h; I, treatment with 0.1  $\mu$ M rotenone for 1 h; CQ group, treatment with 10  $\mu$ M coenzyme 10 for 2 h; PCQ group, treatment with 100  $\mu$ M propofol for 3 h + 10  $\mu$ M coenzyme 10 for 2 h.

cell suspension was centrifuged at 500 x g for 5 min at room temperature, the supernatant was removed, and cells were resuspended using 0.3 ml of PBS.

JC-1 exists as a monomer at low concentrations and as a polymer at high concentrations. Consequently, the emission spectra of these two forms are different and can facilitate the estimation and detection of changes in mitochondrial membrane potential. When mitochondrial membrane potential was increased, the JC-1 polymers increased and the ratio of FL-2/FL-1 also increased. In contrast, when mitochondrial membrane potential decreased, JC-1 monomers increased and FL-2/FL-1 ratios decreased.

**ROS and ATP level analyses.** First, we detected mitochondrial ROS levels using a Beyotime molecular kit (S0033S; Beyotime Institute of Biotechnology). The 2',7'-dichlorofluorescein diacetate (DCFH-DA) probe has no fluorescence and can freely cross the cell membrane. Post cell entry, DCFH-DA can be hydrolyzed by esterases to produce DCFH. However, DCFH itself cannot penetrate the cell wall membrane, which makes this probe easy to assess by loading into cells. Particularly, ROS in cells can oxidize non-fluorescent DCFH to generate fluorescent DCFs. Thus, the level of intracellular ROS can be estimated by detecting the DCF fluorescence. Second, we detected mitochondrial ATP content using spectrophotometry following the manufacturer's protocols (S0026; Beyotime Institute of Biotechnology). Procedures were carried out following all protocols in the molecular kits used.

**Statistical analyses.** Data are expressed as means  $\pm$  standard deviations (SDs) and were analyzed using the Statistical Package for the Social Sciences (SPSS, version 18.0; IBM Corp.). One-way ANOVA was used for comparisons between groups, and a  $P < 0.050$  was considered statistically significant.

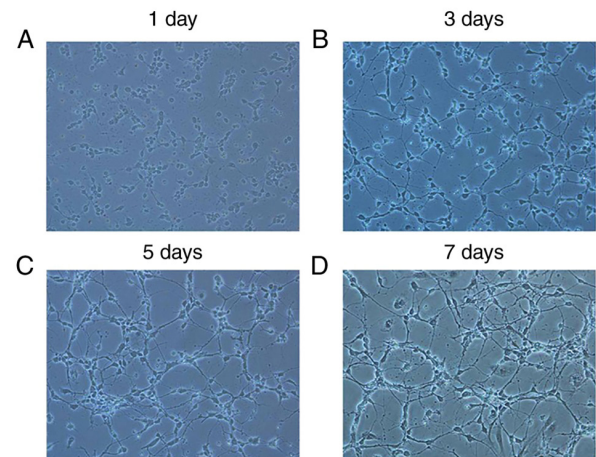


Figure 2. Changes in the morphology of primary hippocampal neurons under light microscopy. (A) One day (24 h) after plating, the halos of the cells were clear, and two to three small dendrites of different lengths extended from the cell body. (B and C) After 3-5 days, the cell body enlarged, the dendrites became thicker and longer, forming a simple neural network. (D) Seven days after culture, the dendritic connections between neurons were more closely linked, with interwoven protrusions forming a more complex neural network.

## Results

**Mitochondrial damage is induced by propofol in a dose-dependent manner.** The experimental processes are represented in Fig. 1. The morphological changes of primary hippocampal neurons from days 1-7 were shown (Fig. 2). Dendritic growth was observed through positive anti-NSE immunocytochemical staining of the cell cytoplasm with the nuclei stained blue (Fig. 3). The effects of propofol on ATP and ROS levels in primary hippocampal neurons are presented in Fig. 4A and B. No significant differences in ATP and ROS levels between C, F and P1 groups were detected ( $P > 0.05$ ). In contrast, compared with the C group, the ATP content was significantly decreased and the ROS content was significantly increased in the P10 and P100 groups ( $P < 0.05$ ). These results showed that the ROS content increased and ATP content decreased with increasing propofol concentrations. Therefore, the mitochondrial damage caused by propofol was found to be concentration-dependent below 100  $\mu$ M (Fig. 4A and B).

**Propofol mediates neuronal apoptosis.** No significant differences were detected in the relative expression levels of Bcl-2, Apaf-1, Bax, cleaved caspase-9, and CytC proteins between the F, D and CQ groups compared with the C group ( $P > 0.05$ ). On the other hand, the Bcl-2 protein content was significantly decreased in the P and I groups, and Apaf-1, Bax, cleaved caspase-9, and CytC were significantly increased in the P group compared with the C group ( $P < 0.050$ ). Additionally, for the PCQ group, the Bcl-2 protein content was significantly increased, and Apaf-1, Bax, cleaved caspase-9, and CytC were significantly decreased compared with the P group ( $P < 0.05$ ) (Fig. 5).

**Neurotoxic effects mediated by propofol are partially inhibited by respiratory chain recovery.** The ATP and ROS content determination results demonstrated a lack of significant differences between the F, D and CQ groups ( $P > 0.05$ ),

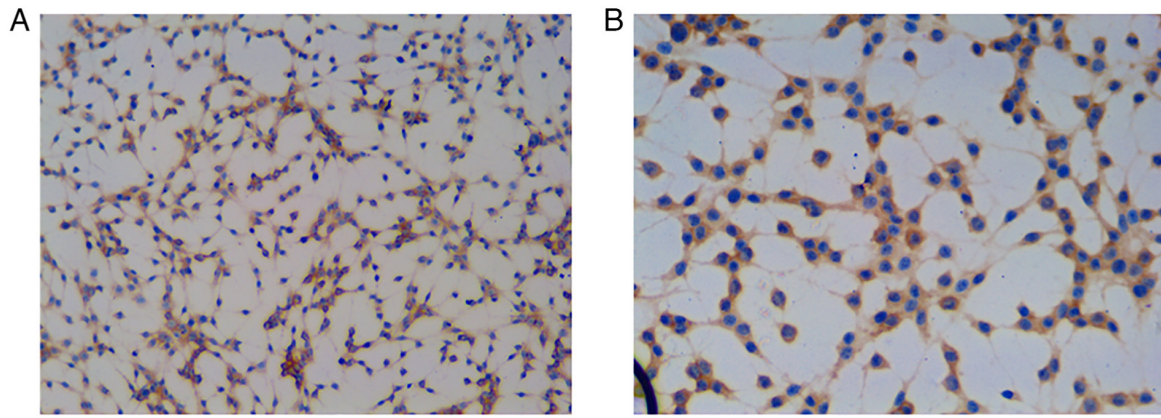


Figure 3. Primary hippocampal neurons (7 DIV) were identified by anti-NSE immunocytochemical staining, and a purity analysis was performed. (A and B) After staining with rabbit monoclonal antibody against neuron-specific enolase (NSE), under light microscope, the hippocampal neuronal cell bodies, dendrites, and axons were brown, and the axons and dendrites formed synaptic connections between the cells in a reticular pattern. The nuclei were blue-stained with DAPI. Thus, rat hippocampal neuronal cells were successfully cultured *in vitro*. The proportion of NSE-positive hippocampal neurons among the total number of cells in the visual field was counted in eight fields of view. The purity of hippocampal neurons was  $92.2 \pm 1.6\%$  ( $n=8$  fields). 7 DIV, 7 days *in vitro*.

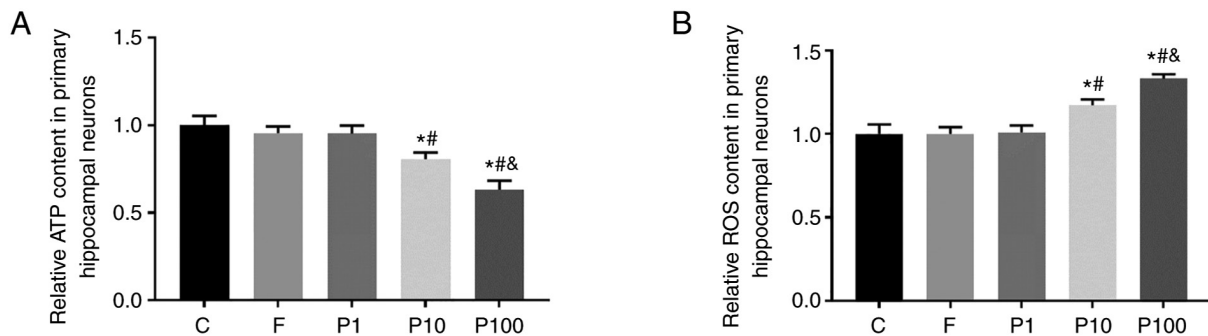


Figure 4. Mitochondrial damage was induced by propofol in a dose-dependent manner. (A) ATP and (B) ROS levels were detected after primary neurons were treated.  $n=3$ ,  $^*P<0.05$  compared with the C group;  $^{\#}P<0.05$  compared with the P1 group;  $^{\&}P<0.05$  compared with the P10 group. C, Control group; F, Fat emulsion group; P1, 1  $\mu\text{M}$  propofol group; P10, 10  $\mu\text{M}$  propofol group; P100, 100  $\mu\text{M}$  propofol group.

whereas ATP and ROS contents in I groups were significantly decreased compared to the control ( $P<0.05$ ). Compared with the P group, ATP contents were significantly increased in the PCQ group while ROS group significantly decreased in the PCQ group ( $P<0.05$ ) (Fig. 6A and B).

Moreover, we measured the mitochondrial membrane potential. Our findings indicated that, compared with the C group, no significant differences in mitochondrial membrane potential were found between the F and D groups ( $P>0.05$ ). On the other hand, compared with group C, the mitochondrial membrane potential was significantly increased in the CQ group ( $P<0.05$ ) and significantly decreased in the P and I groups ( $P<0.05$ ). The mitochondrial membrane potential was significantly increased in the PCQ group compared with the P group ( $P<0.05$ ; Fig. 6C and D).

Altogether, these results suggest that propofol may cause neuronal apoptosis and neurotoxicity by inducing mitochondrial membrane potential inhibition.

## Discussion

Propofol is a fast and short-acting intravenous anesthetic widely used in clinical anesthesia and ICU sedation (16-18). Since Patel and Knights (19) discovered in 1992 that

pediatric behavioral abnormalities were caused by propofol anesthesia at clinical doses, many animal and cell-based experiments have been used to investigate whether or not propofol induces neurotoxicity in developing brain. For example, clinical doses of propofol injected into newborn mice for 5 or 7 days increased apoptotic neuron numbers in developing brains and caused abnormal development of the central nervous system. These effects continued through adulthood, subsequently affecting various neurological processes (20).

In the present study, we established an *in vitro* model of hippocampal neurons. We incubated propofol at different concentrations with primary neurons to simplify otherwise complex biological processes. The effects of propofol on the survival, growth, development, morphological function and molecular neuronal dynamics were assessed, increasing the knowledge regarding its molecular mechanisms. Our current findings indicated that propofol inhibited the growth of hippocampal neurons in a dose-dependent manner. Compared with the control group, the inhibition of hippocampal neurons was most significant for the propofol 100  $\mu\text{M}$  group. Additionally, propofol incubation significantly increased the levels of hippocampal neuron apoptotic proteins. These results indicated that propofol promoted cell apoptosis.



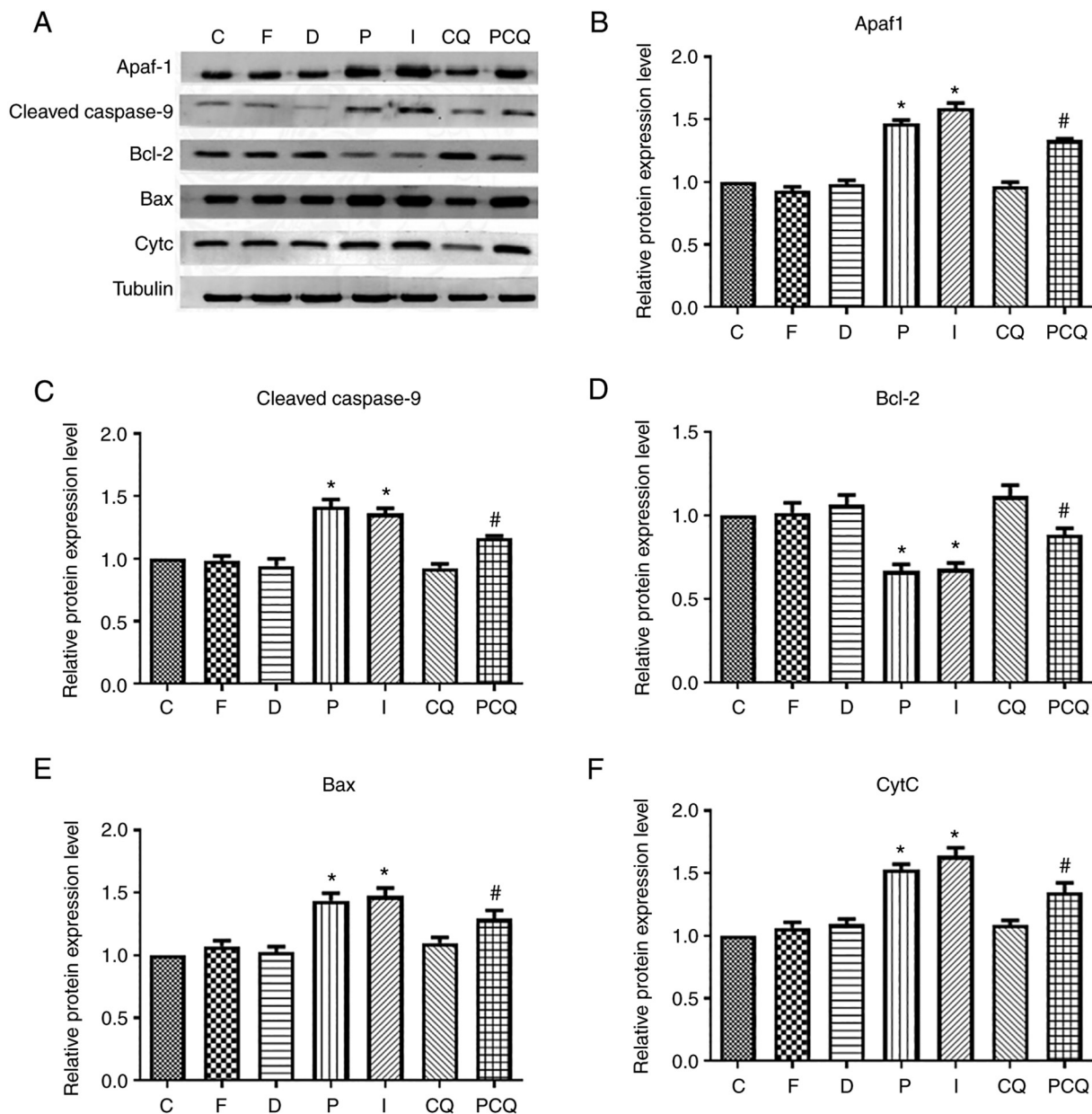


Figure 5. Propofol mediates neuronal apoptosis. After treatment of cells in the indicated groups, cleaved caspase-9, cytochrome c (CytC), Bax, Apaf-1, and Bcl-2 were detected by western blotting. Representative bands (A) and histograms (B-F). n=3, \*P<0.05 compared with the C group; #P<0.05 compared with the P group. C, Control group; F, Fat emulsion group; D, 0.25% DMSO; P, treatment with 100  $\mu$ M propofol for 3 h; I, treatment with 0.1  $\mu$ M rotenone for 1 h; CQ group, treatment with 10  $\mu$ M coenzyme 10 for 2 h; PCQ group, treatment with 100  $\mu$ M propofol for 3 h + 10  $\mu$ M coenzyme 10 for 2 h.

In immature neurons, propofol is a GABA receptor stimulant, and high propofol concentrations can directly activate GABA receptors, which in turn activate NMDA receptors (21). Additionally, high concentrations (500  $\mu$ mol/l) of propofol can increase lysosomal membrane permeability of macrophages and vascular endothelial cells, facilitate sustained depolarization of mitochondrial membrane potential, induce oxidative phosphorylation uncoupling, and decrease intracellular ATP concentrations, ultimately leading to macrophage and vascular endothelial cell necrosis (22). Therefore, high concentrations of propofol might also cause neuronal necrosis by acting directly on lysosomes and mitochondria.

Propofol is also known to affect the activity of hippocampal neurons and promote their apoptosis, which may also be related to the abnormal expression of different intracellular proteins.

Nuclear factor (NF)- $\kappa$ B is a DNA-binding protein that triggers gene expression of various inflammatory mediators, such as tumor necrosis factor (TNF)- $\alpha$ , and promotes transcription of genes associated with cell proliferation (23). For example, decreased expression of NF- $\kappa$ B can promote neuronal apoptosis since NF- $\kappa$ B can counteract apoptotic programming by regulating the Bcl-2 protein family that inhibits apoptosis (24). On the other hand, NF- $\kappa$ B can directly act upon the ultimate executor of apoptosis, thereby blocking apoptosis by reducing downstream caspase-3 activity. Under normal circumstances, caspase-3 exists in a prototype form in cells (25). When apoptotic signals act on cell receptors, caspase-3 becomes activated and hydrolyzes intracellular substrates, finally leading to cell apoptosis. A previous study showed that 25 mg/kg propofol overactivated TNF in neurons of newborn 5-day-old mice, which

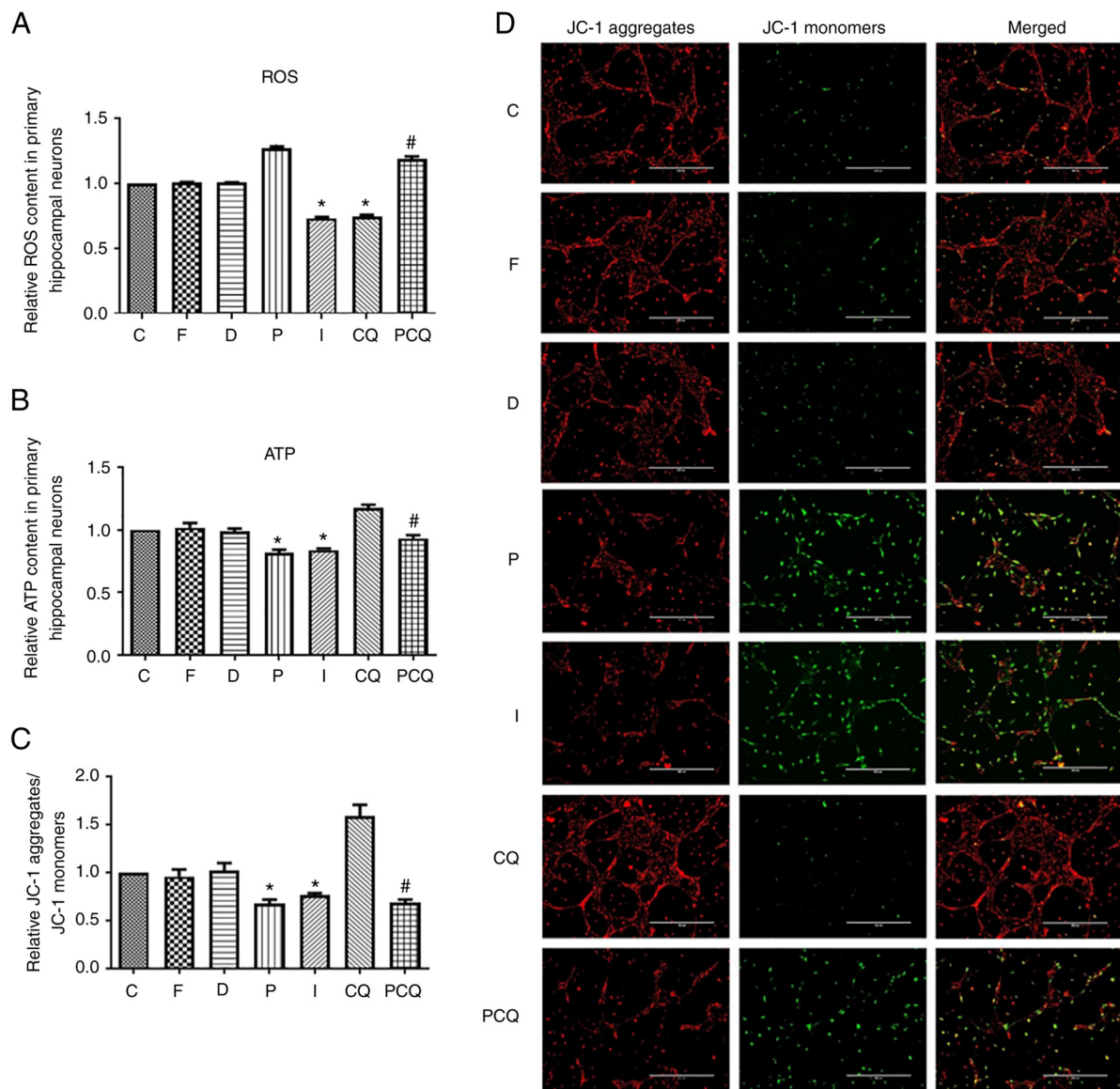


Figure 6. Neurotoxic effects mediated by propofol are partially inhibited by respiratory chain recovery. After treatment of cells in the indicated groups, (A) ATP, (B) ROS, and (C) mitochondrial membrane potential were detected. (D) Representative mitochondrial membrane potential results are shown. When the mitochondrial membrane potential is high, JC-1 can gather in the mitochondrial matrix to form red fluorescent polymers (J-aggregates). When the mitochondrial membrane potential is low, JC-1 can not gather in the mitochondrial matrix, remaining a green fluorescent monomer.  $n=3$ , \* $P<0.05$  compared with the C group; # $P<0.05$  compared with the P group. C, Control group; F, Fat emulsion group; D, 0.25% DMSO; P, treatment with 100  $\mu$ M propofol for 3 h; I, treatment with 0.1  $\mu$ M rotenone for 1 h; CQ group, treatment with 10  $\mu$ M coenzyme 10 for 2 h; PCQ group, treatment with 100  $\mu$ M propofol for 3 h + 10  $\mu$ M coenzyme 10 for 2 h.

in turn activated caspase-3, leading to extensive neuronal cell apoptosis. Moreover, 3 or 5  $\mu$ M propofol significantly increased intracellular activated caspase-3 protein in hippocampal neurons cultured *in vitro* over 4-7 days (26). The increased expression of caspase-3 in the 1,000  $\mu$ M propofol group might have been related to cell necrosis. Programmed cell necrosis pathways were found to be activated under various death signals (27). Mitochondrial inner membrane permeability, transition pore development, and lysosomal membrane permeability increased when cytochrome *c* (CytC), cathepsin, and other proteins are released into the cytoplasm. These activated apoptosis-related proteins in the Bcl and caspase families can increase the expression of apoptosis-related proteins in the cytoplasm.

Mitochondria are the main sites where eukaryotic cells carry out biological oxidation which is accompanied by ROS

production (28). When ROS are overproduced, oxidative stress responses in hippocampal neurons are increased and can lead to apoptosis (29,30). Apoptosis of hippocampal neurons is an important mechanism that maintains homeostasis in the brain, and mitochondrial apoptosis is one of the important pathways in this process (31). Increased activity and expression of caspase-3 and caspase-9 are considered markers of mitochondrial apoptotic pathways activity (32). However, the effects of propofol upon mitochondrial oxidative stress-related apoptotic pathways have rarely been examined. Previous research indicated that propofol could reduce hippocampal neuronal apoptosis after ischemia-reperfusion in rats, which may be related to the activation of the PI3K/AKT signaling pathway and upregulation of Bcl-2 protein expression, exerting neuroprotective effects (32). Since the prior maximum plasma concentration of propofol

used clinically is 56  $\mu$ M, we selected 100  $\mu$ M as the highest experimental concentration in our assessments (33). We examined the effects of propofol-induced oxidative stress injuries on reactive oxygen species (ROS) and ATP levels, and apoptosis in hippocampal neurons. Previous studies (34,35) have shown that propofol could increase mitochondrial ROS levels, decrease ATP levels, and increase mitochondrial-mediated activation of Apaf-1, cleaved caspase-9, and CytC apoptotic factors in hippocampal neurons, ultimately leading to hippocampal neuronal apoptosis. Respiratory chain inhibitors can have similar effects, which suggests that propofol might act on the mitochondrial respiratory chain (36). Additionally, in the present study, the respiratory chain activator was able to reverse propofol-induced mitochondrial oxidative stress injuries to some extent, as well as induce increased ATP levels, and decrease ROS and mitochondrial apoptotic pathway-related factors, including Apaf-1, cleaved caspase-9 and CytC.

Our current results also indicated that propofol could mediate damage and apoptosis of hippocampal neurons by inhibiting the mitochondrial membrane potential and regulating mitochondrial apoptotic pathways. Moreover, these findings demonstrated that ROS levels in the 1  $\mu$ M propofol group did not significantly change compared with the control group. This result demonstrated that propofol increased ROS basal levels in a dose-dependent manner. Respiratory chain inhibitors can also induce increased ROS production in hippocampal neurons, resulting in excessive ROS accumulation. In addition, excessive ROS can cause mitochondrial redox imbalance, leading to the activation of mitochondrial apoptotic pathways and apoptosis. Respiratory chain activators relieved oxidative stress load and inhibited intracellular ROS production, Apaf-1, cleaved caspase-9, and CytC in hippocampal neurons treated with propofol.

Overall, propofol induced neuronal apoptosis and facilitated neurotoxicity by inhibiting mitochondrial membrane potential. However, whether or not propofol might also exert neurotoxicity through other pathways and the specific dynamics underlying the signal transduction mechanisms require further studies.

## Acknowledgements

Not applicable.

## Funding

This study was supported by the Natural Science Foundation of Guangxi (2017GXNSFBA198108), the Youth Fund of Guangxi Medical University (GXMUYSF201518), and Guangxi Key R&D Projects (AB18126061).

## Availability of data and materials

The datasets used and/or analyzed during the current study are available from the corresponding author on reasonable request.

## Authors' contributions

YL and LP contributed to conception or design of the work; YH and RS wrote the manuscript; FX, FL, RS and HD reviewed

and edited the manuscript; LP, RS and FL performed the data analysis; YL, YH, FX, FL and HD performed the experiments. All authors read and approved the manuscript and agreed to be accountable for all aspects of the research in ensuring that the accuracy or integrity of any part of the work are appropriately investigated and resolved. YL and LP confirm the authenticity of all the raw data. All authors read and approved the final manuscript.

## Ethics approval and consent to participate

The experimental procedures and protocols were approved by the Animal Use and Care Committee of the Guangxi Medical University (no. SCXK GUI 2004-0002) and were performed following the Guangxi Medical University's guidelines for Ethical Review of Animal Welfare (approval number 201807366).

## Patient consent for publication

Not applicable.

## Competing interests

The authors declared that there are no competing interests.

## References

1. Carvalho C, Correia S, Santos MS, Seica R, Oliveira CR and Moreira PI: Metformin promotes isolated rat liver mitochondria impairment. *Mol Cell Biochem* 308: 75-83, 2008.
2. Boulghobra D, Grillet PE, Laguerre M, Tenon M, Fauconnier J, Faucha-Berthon P, Reboul C and Cazorla O: Sinapine, but not sinapic acid, counteracts mitochondrial oxidative stress in cardiomyocytes. *Redox Biol* 34: 101554, 2020.
3. Wang Y, Qian M, Qu Y, Yang N, Mu B, Liu K, Yang J, Zhou Y, Ni C, Zhong J and Guo X: Genome-wide screen of the hippocampus in aged rats identifies mitochondria, metabolism and aging processes implicated in sevoflurane anesthesia. *Front Aging Neurosci* 12: 122, 2020.
4. Urban T, Waldauf P, Krajčová A, Jiroutková K, Halačová M, Džupa V, Janoušek L, Pokorná E and Duška F: Kinetic characteristics of propofol-induced inhibition of electron-transfer chain and fatty acid oxidation in human and rodent skeletal and cardiac muscles. *PLoS One* 14: e0217254, 2019.
5. Rigoulet M, Devin A, Avéret N, Vandais B and Guérin B: Mechanisms of inhibition and uncoupling of respiration in isolated rat liver mitochondria by the general anesthetic 2, 6-diisopropylphenol. *Eur J Biochem* 241: 280-285, 1996.
6. Vasile B, Rasulo F, Candiani A and Latronico N: The pathophysiology of propofol infusion syndrome: A simple name for a complex syndrome. *Intensive Care Med* 29: 1417-1425, 2003.
7. Guitton C, Gabillet L, Latour P, Rigal JC, Boutoille D, Al Habash O, Derkinderen P, Bretonniere C and Villers D: Propofol infusion syndrome during refractory status epilepticus in a young adult: Successful ECMO resuscitation. *Neurocrit Care* 15: 139-145, 2011.
8. Santucci R, Sinibaldi F, Cozza P, Polticelli F and Fiorucci L: Cytochrome c: An extreme multifunctional protein with a key role in cell fate. *Int J Biol Macromol* 136: 1237-1246, 2019.
9. Guerra-Castellano A, Díaz-Quintana A, Pérez-Mejías G, Elena-Real CA, González-Arzoila K, García-Mauriño SM, De la Rosa MA and Díaz-Moreno I: Oxidative stress is tightly regulated by cytochrome c phosphorylation and respirasome factors in mitochondria. *Proc Natl Acad Sci USA* 115: 7955-7960, 2018.
10. Chimenti MS, Sunzini F, Fiorucci L, Botti E, Fonti GL, Conigliaro P, Triggianese P, Costa L, Caso F, Giunta A, *et al*: Potential role of cytochrome c and tryptase in psoriasis and psoriatic arthritis pathogenesis: Focus on resistance to apoptosis and oxidative stress. *Front Immunol* 9: 2363, 2018.



11. Li P, Nijhawan D, Budihardjo I, Srinivasula SM, Ahmad M, Alnemri ES and Wang X: Cytochrome c and dATP-dependent formation of Apaf-1/caspase-9 complex initiates an apoptotic protease cascade. *Cell* 91: 479-489, 1997.
12. Fang X, Miao XL, Liu JL, Zhang DW, Wang M, Zhao DD, Mu QQ, Yu N, Mo FF, Yin HP and Gao SH: Berberine induces cell apoptosis through cytochrome C/apoptotic protease-activating factor 1/caspase-3 and apoptosis inducing factor pathway in mouse insulinoma cells. *Chin J Integr Med* 25: 853-860, 2019.
13. Zhang L, Cheng X, Xu S, Bao J and Yu H: Curcumin induces endoplasmic reticulum stress-associated apoptosis in human papillary thyroid carcinoma BCPAP cells via disruption of intracellular calcium homeostasis. *Medicine (Baltimore)* 97: 1-5, 2018.
14. Zhang F, Xiang S, Cao Y, Li M, Ma Q, Liang H, Li H, Ye Y, Zhang Y, Jiang L, *et al*: EIF3D promotes gallbladder cancer development by stabilizing GRK2 kinase and activating PI3K-AKT signaling pathway. *Cell Death Dis* 8: e2868, 2017.
15. Iijima T, Mishima T, Akagawa K and Iwao Y: Neuroprotective effect of propofol on necrosis and apoptosis following oxygen-glucose deprivation-relationship between mitochondrial membrane potential and mode of death. *Brain Res* 1099: 25-32, 2006.
16. Takamatsu I, Sekiguchi M, Wada K, Sato T and Ozaki M: Propofol-mediated impairment of CA1 long-term potentiation in mouse hippocampal slices. *Neurosci Lett* 389: 129-132, 2005.
17. Veselis RA, Reinsel RA, Wroński M, Marino P, Tong WP and Bedford RF: EEG and memory effects of low-dose infusions of propofol. *Br J Anaesth* 69: 246-254, 1992.
18. Erasso DM, Chaparro RE, Quiroga Del Rio CE, Karlinski R, Camporesi EM and Saporta S: Quantitative assessment of new cell proliferation in the dentate gyrus and learning after isoflurane or propofol anesthesia in young and aged rats. *Brain Res* 1441: 38-46, 2012.
19. Patel P and Knights DT: Abnormal movements following recovery from propofol, alfentanil and nitrous oxide anaesthesia. *Anaesthesia* 47: 442-443, 1992.
20. Widestrand A, Fajerson J, Wilhelmsson U, Smith PL, Li L, Sihlbom C, Eriksson PS and Pekny M: Increased neurogenesis and astrogenesis from neural progenitor cells grafted in the hippocampus of GFAP<sup>-/-</sup> Vim<sup>-/-</sup> mice. *Stem Cells* 25: 2619-2627, 2007.
21. Hsing CH, Chen YH, Chen CL, Huang WC, Lin MC, Tseng PC, Wang CY, Tsai CC, Choi PC and Lin CF: Anesthetic propofol causes glycogen synthase kinase-3 $\beta$ -regulated lysosomal/mitochondrial apoptosis in macrophages. *Anesthesiology* 116: 868-881, 2012.
22. Lin MC, Chen CL, Yang TT, Choi PC, Hsing CH and Lin CF: Anesthetic propofol overdose causes endothelial cytotoxicity in vitro and endothelial barrier dysfunction in vivo. *Toxicol Appl Pharmacol* 265: 253-262, 2012.
23. Dong WB, Hou HM, Wang Q, Chen F and Hang YL: NF-kappaB-mediated protective effect of erythropoietin on neuron against glutamate-induced damage. *Xi Bao Yu Fen Zi Mian Yi Xue Za Zhi* 24: 584-585, 2008 (In Chinese).
24. Wang Y, Wang X, Zhao H, Liang B and Du Q: Clusterin confers resistance to TNF-alpha-induced apoptosis in breast cancer cells through NF-kappaB activation and Bcl-2 overexpression. *J Chemother* 24: 348-357, 2012.
25. Suzuki Y, Nakabayashi Y and Takahashi R: Ubiquitin-protein ligase activity of X-linked inhibitor of apoptosis protein promotes proteasomal degradation of caspase-3 and enhances its anti-apoptotic effect in Fas-induced cell death. *Proc Natl Acad Sci USA* 98: 8662-8667, 2001.
26. Yu D, Jiang Y, Gao J, Liu B and Chen P: Repeated exposure to propofol potentiates neuroapoptosis and long-term behavioral deficits in neonatal rats. *Neurosci Lett* 534: 41-46, 2013.
27. Garvin AM, Jackson MA and Korzick DH: Inhibition of programmed necrosis limits infarct size through altered mitochondrial and immune responses in the aged female rat heart. *Am J Physiol Heart Circ Physiol* 315: H1434-H1442, 2018.
28. Guzy RD and Schumacker PT: Oxygen sensing by mitochondria at complex III: The paradox of increased reactive oxygen species during hypoxia. *Exp Physiol* 91: 807-819, 2006.
29. Ullah I, Park HY and Kim MO: Anthocyanins protect against kainic acid-induced excitotoxicity and apoptosis via ROS-activated AMPK pathway in hippocampal neurons. *CNS Neurosci Ther* 20: 327-338, 2014.
30. Yu AR, Jeong YJ, Hwang CY, Yoon KS, Choe W, Ha J, Kim SS, Pak YK, Yeo EJ and Kang I: Alpha-naphthoflavone induces apoptosis through endoplasmic reticulum stress via c-Src-, ROS-, MAPKs-, and arylhydrocarbon receptor-dependent pathways in HT22 hippocampal neuronal cells. *Neurotoxicology* 71: 39-51, 2019.
31. Zhou X, Yong L, Huang Y, Zhu S, Song X, Li B, Zhu J and Wang H: The protective effects of distal ischemic treatment on apoptosis and mitochondrial permeability in the hippocampus after cardiopulmonary resuscitation. *J Cell Physiol* 233: 6902-6910, 2018.
32. Yang YJ, Qi SN, Shi RY, Yao J, Wang LS, Yuan HQ and Jing YX: Induction of apoptotic DNA fragmentation mediated by mitochondrial pathway with caspase-3-dependent BID cleavage in human gastric cancer cells by a new nitroxyl spin-labeled derivative of podophyllotoxin. *Biomed Pharmacother* 90: 131-138, 2017.
33. Mohler T, Welter J, Steurer M, Neumann L, Zueger M, Kraemer T and Dullenkopf A: Measuring the accuracy of propofol target-controlled infusion (TCI) before and after surgery with major blood loss. *J Clin Monit Comput* 34: 97-103, 2020.
34. Ma H, Liu Y, Li Z, Yu L, Gao Y, Ye X, Yang B, Li H and Shi J: Propofol protects against hepatic ischemia reperfusion injury via inhibiting Bnip3-mediated oxidative stress. *Inflammation* 44: 1288-1301, 2021.
35. Zhang HS, Liu CD, Zheng MC, Zhao HT and Liu XJ: Propofol alleviates hypoxic neuronal injury by inhibiting high levels of mitochondrial fusion and fission. *Eur Rev Med Pharmacol Sci* 24: 9650-9657, 2020.
36. Berndt N, Rösner J, Haq RU, Kann O, Kovács R, Holzhütter HG, Spies C and Liotta A: Possible neurotoxicity of the anesthetic propofol: Evidence for the inhibition of complex II of the respiratory chain in area CA3 of rat hippocampal slices. *Arch Toxicol* 92: 3191-3205, 2018.



This work is licensed under a Creative Commons Attribution-NonCommercial-NoDerivatives 4.0 International (CC BY-NC-ND 4.0) License.